Observation of subwavelength localization of cavity plasmons induced by ultra-strong exciton coupling

M. Balasubrahmaniyam, Durgesh Kar, Prabal Sen, Prem B. Bisht, and S. Kasiviswanathan

Citation: Appl. Phys. Lett. **110**, 171101 (2017); doi: 10.1063/1.4979838
View online: http://dx.doi.org/10.1063/1.4979838
View Table of Contents: http://aip.scitation.org/toc/apl/110/17
Published by the American Institute of Physics

Observation of subwavelength localization of cavity plasmons induced by ultra-strong exciton coupling

M. Balasubrahmaniyam,[1,a)] Durgesh Kar,[2] Prabal Sen,[2] Prem B. Bisht,[2] and S. Kasiviswanathan[2,b)]
[1]*Nano-optics and Mesoscopic Optics Laboratory, Tata Institute of Fundamental Research, 1, Homi Bhabha Road, Mumbai 400 005, India*
[2]*Department of Physics, Indian Institute of Technology Madras, Chennai 600 036, India*

(Received 20 December 2016; accepted 26 March 2017; published online 24 April 2017)

In condensed matter systems, there exists a class of exotic localized electronic states wherein the localization is induced, not by a disorder or a defect, but by extremely strong interactions, for example, Kondo-insulator and Mott-insulator. In this work, we investigate and experimentally implement the photonic analog of localization induced by ultra-strong interactions in a coupled three-mode system. We show that the localization of a propagating mode can be achieved without the aid of an underlying spatial disorder, a defect, or even periodicity. We demonstrate the same by realizing ultra-strong coupling between a highly dispersive cavity plasmon mode and dimer excitons of Rhodamine B. Using a photon tunneling arrangement, we map the dispersion of the hybrid modes and provide evidence for the existence of a quasi-dispersionless hybrid mode with the sub-wavelength localization length and cavity plasmon-like characteristics. *Published by AIP Publishing.*
[http://dx.doi.org/10.1063/1.4979838]

Following the pioneering work by Phillip Anderson in 1958, which showed that the coherent scattering in a disordered system can stop the transport, engineering of localized states that prevent the propagation of light has attracted a lot of attention.[1] Such localization effects typically depend on the dimensionality, the presence of disorder, and the nature of interactions. Intense research in this field has resulted in novel applications such as random lasing and sheds light on the fundamental processes involved.[2] Usually, some form of defect, linear or nonlinear, point-like or extended, or disorder, has been used for achieving the localization of modes. However, defects are not prerequisites, as they are the destructive wave interferences that lead to localization.[3–5] In general, a localized mode would translate into a flat-dispersive or a quasi-dispersionless energy band with degenerate (momentum) states, the superposition of which displays no group velocity or any other contribution from the higher order derivatives of frequency with respect to the wave number (i.e., no dynamical evolution). Essentially, the large degeneracy results in a large number of wavelets being added in Fourier space which reflects in real space as the localization of the mode. Therefore, larger degeneracy implies shorter spatial extent for the mode. In this work, we show that quasi-dispersionless modes can be realized, without the aid of an underlying spatial disorder, a defect, or even periodicity, by establishing ultra-strong coupling in a three mode system with a certain configuration. An electronic counterpart of such strong interaction induced localization has been studied in condensed matter systems such as Kondo-insulators, Mott-insulators, and multi-layered quantum wells. Unlike disorder or defect induced localization, the studies on the photonic analog of localization due to strong interactions have been limited to the recent observation of localization in a Lieb photonic lattice, independently by Thomson and Molina.[6,7] We experimentally demonstrate the interaction induced localization in an entirely different system: in a system of a highly dispersive cavity plasmon mode and two exciton modes, by achieving ultra-strong coupling. As the localization mechanism is based on strong interactions alone, the minimum achievable localization length is not limited by length scales like the distance between the scatterers (in Anderson localization) or the special periodicity (in a Lieb photonic lattice) and therefore allows us to achieve sub-wavelength localization. We map the dispersion characteristics of the hybrid states using a photon tunneling arrangement and show that in the ultra-strong coupling limit, a localized hybrid mode with the subwavelength localization length, and with cavity plasmon-like characteristics, emerges. Such a strong localized exciton-plasmon hybrid mode is also important in lasing and plasmon amplification applications.

To demonstrate the localization effect introduced by ultra-strong coupling in a three-mode system, we consider a coupled system with three lossless modes $|a_1\rangle$ and $|a_2\rangle$ with the non-dispersive Eigenvalues E_1 and E_2, respectively, and $|a_0\rangle$ with a linearly dispersive Eigenvalue E_0. Coupling is such that the modes $|a_1\rangle$ and $|a_2\rangle$ are coupled to the mode $|a_0\rangle$, but there is no direct coupling between themselves. The Hamiltonian for such a system can be written as

$$H = \begin{pmatrix} E_1 & g & 0 \\ g & E_0(k) & g \\ 0 & g & E_2 \end{pmatrix}, \tag{1}$$

where g determines the coupling (time-independent) between $|a_0\rangle$ and the modes $|a_1\rangle$ and $|a_2\rangle$. Since the modes are taken to be loss-less, for any non-zero g, the system will be in the strong coupling limit. Therefore, two individual avoided crossing points will appear in the dispersion, as shown by the continuous lines in Fig. 1(a). In this case, the system may be

a)Present address.
b)Electronic mail: kasi@iitm.ac.in

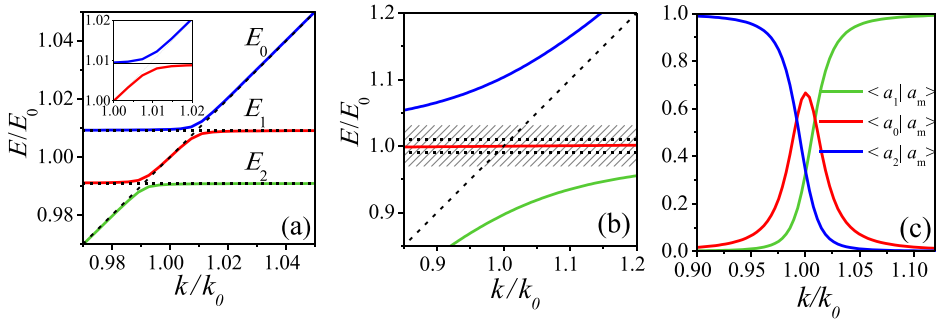

FIG. 1. (a) Dispersion of a three-mode coupled system in the strong coupling limit, with the inset showing the dispersion of the reduced two-mode coupled system. (b) Dispersion of the same in the ultra-strong coupling limit. The dashed lines depict the dispersion of the uncoupled modes. The shaded region shows the permanent gap opened up due to the ultra-strong coupling. (c) The fractional contribution of the uncoupled modes to the quasi-dispersionless mode in the irreducible three-mode coupled system.

treated as two independent systems with associated Rabi splitting.[8] As an example, the Eigenvalues of the strongly coupled two-mode Hamiltonians close to the point where $|a_0\rangle$ and $|a_1\rangle$ are degenerate, as shown in the inset of Fig. 1(a).

However, when g becomes a substantial fraction of other energy scales in the system, certain interesting phenomena emerge.[9,10] In the present case, another energy scale $(E_1 - E_2)$, other than the decay, gets introduced automatically, and as a result, the coupling between these three modes becomes irreducible in the limit $g \rightarrow (E_1 - E_2)/2$. In other words, when $g \geq (E_1 - E_2)/2$, the system has to be treated as an irreducible three-mode coupled system as shown in Fig. 1(b), for the case $g = 2 * (E_1 - E_2)$. The dispersion here shows an upper and a lower mode with hyperbolic dispersion and Rabi-splitting similar to the two-mode coupled system. However, unlike in the case of a two mode system wherein the Eigenvalues tend to approach the uncoupled mode values asymptotically away from Rabi splitting (Fig. 1(a)), a permanent gap between the upper and lower modes opens up (Fig. 1(b)). Such a coupling behavior is known as ultra-strong coupling, and a range of new physical phenomena have been predicted, which include parametric generation of non-classical light upon strong modulation of carrier density.[11,12]

Nevertheless, the primary interest here is the quasi-dispersionless third mode (denoted, $|a_m\rangle$) that appears at the middle of the gap. On the first look, this mode seems to be similar to the uncoupled modes $|a_1\rangle$ and $|a_2\rangle$. However, for further understanding the nature of $|a_m\rangle$, the fractional contribution (mixing fraction) of the uncoupled modes to $|a_m\rangle$: $\langle a_1|a_m\rangle$, $\langle a_2|a_m\rangle$, and $\langle a_0|a_m\rangle$ is calculated (Fig. 1(c)). Fig. 1(c) shows that the contribution from $|a_1\rangle$ and $|a_2\rangle$ (green and blue curves) dominates away from the Rabi splitting. In contrast, the contribution from the dispersive mode $|a_0\rangle$ (red curve in Fig. 1(c)) dominates close to Rabi splitting and vanishes away from the splitting region. This implies that the hybrid mode $|a_m\rangle$ exhibits characteristics of the dispersive uncoupled mode $|a_0\rangle$ close to Rabi splitting while being quasi-dispersionless or, as discussed earlier, localized. This opens up a possibility of engineering a localized hybrid mode with the characteristics of dispersive modes like $|a_0\rangle$ close to the Rabi-splitting.

The coupling strength, in general, is determined by the extent of the overlap between the modes involved in coupling. Since the length scales associated with electronic excitations are smaller than that of photonic modes by at least two orders of magnitude, the coupling strength in hybrid systems like the photon-exciton system will be determined solely by the mode volume of the photonic mode. The mode volume associated with cavity plasmons can be reduced to extremely small values.[13] This makes cavity plasmon-exciton hybrid systems an exceptionally good choice for achieving ultra-strong coupling and for observing aforementioned effects. Cavity-plasmons themselves are coupled modes of two identical surface plasmon modes, and as a result, they have a highly nonlinear dispersion.[14,15] Of the two coupled cavity plasmon modes, we use the antisymmetric plasmon (ASP) mode to couple with excitonic modes as their dispersion characteristics exhibit large tunability with the cavity size. The ASP mode has a lower cut-off frequency determined by the cavity size along with an upper cut-off frequency originating from the metal plasma frequency. The choice of the dispersionless excitonic levels is determined by the cut-off frequencies associated with the uncoupled ASP mode. We chose the exciton levels of Rhodamine B dissolved in water (refractive index, $n_c = 1.33$) for this purpose. At large concentrations (10^{-3} M), Rhodamine B forms dimer molecules,[16] which results in two distinct excitonic resonances at 2.24 eV and 2.37 eV.

We probe the dispersion characteristics of the hybrid modes using a prism arrangement in a photon tunneling configuration.[17] Here, two prisms (SF11, refractive index ~1.78) with 40 nm thick Ag films coated over their hypotenuse face are brought close to each other to form the cavity, and Fig. 2(a) shows the schematic of the same. In all experiments, the transmitted signal of TM polarized light in the total internal reflection configuration has been measured. For almost all frequencies and angles of incidence, the metallic cavity works as a mirror and the transmitted signal remains negligibly small, except at the coupled mode resonances. At the coupled mode resonances, distinct resonant maxima occur in the transmission due to resonant photon tunneling. The red curve in Fig. 2(b) shows, as an example, the transmittance due to the ASP mode measured at an angle of 48° without the dye (with water) in the cavity. The blue curve in Fig. 2(b) shows the transmittance of Rhodamine B in water and is included for the sake of comparison. The energy difference between the exciton resonances of Rhodamine B is 130 meV, which is well within the lower and upper cut-off frequencies of ASP (1.99 eV and 2.57 eV, respectively).

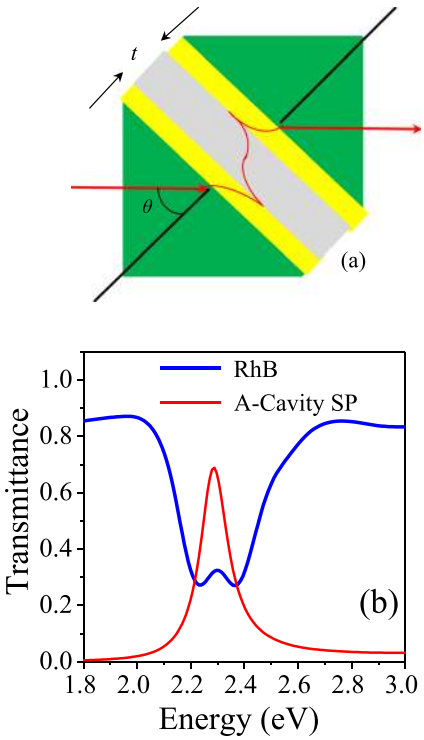

FIG. 2. (a) Schematic of the photon tunneling based configuration. (b) Transmittance of Rhodamine B (blue curve) and the ASP mode. The latter is measured using the tunnel configuration.

The dispersion of the ASP mode calculated for the present configuration is shown in Fig. 3(a) (in grayscale) along with that of the two Rhodamine B excitons (horizontal green and red dashed lines). The Introduction of Rhodamine B into the cavity results in the formation of three ASP-exciton hybrid modes and splits the measured ASP transmission peak into three as shown in Fig. 3(b). Fig. 3(c) shows the position of these peaks in Fig. 3(b) mapped as a function of the angle of incidence. It is clear from Fig. 3(c) that coupling opens up a permanent broad gap of ~420 meV between the upper and lower modes, confirming the ultra-strong coupling between the exciton levels and the ASP mode. More importantly, $|a_m\rangle$ (at 2.31 eV) is effectively quasi-dispersionless (dispersionless within ± 0.004 eV) and shows ASP like transmission maxima of ~40% to 60% over wide range angles of incidence, from 25° to 80°. The upper and lower modes are still dispersive, but the extent of dispersion is lesser than that of the uncoupled ASP mode. To fit the observed results, a three-mode coupled system similar to Eq. (1) with an ASP mode and two exciton modes is used

$$H = \begin{pmatrix} E_1 - i\gamma_{ex} & g_{ep} & 0 \\ g_{ep} & E_{ASP}(\theta) - i\gamma_{ASP} & g_{ep} \\ 0 & g_{ep} & E_2 - i\gamma_{ex} \end{pmatrix}. \quad (2)$$

Here, E_1, E_2, and E_{ASP} are the energies corresponding to the two excitonic excitations and ASP mode. The losses γ_{ex} and γ_{ASP} associated with all the modes are obtained from the measured responses (Fig. 2(b)) and included in the model. The analytical form of the ASP dispersion, $E_{ASP}(\theta)$, can be obtained from that of a TM_0 cavity mode with a lower cut-off frequency E_o after considering the effective index n_{eff}.[18]

$$E_{ASP}(\theta) = 2E_o\sqrt{1 - \frac{\sin(\theta)}{n_{eff}}}, \quad (3)$$

where

$$E_o = \hbar\pi \frac{1}{n_c\left(\frac{2}{\omega_p} + \frac{t}{c}\right)} \text{ and } n_{eff} = \frac{n_c\left(\frac{2c}{\omega_p} + t\right)}{\sqrt{t^2 - \left(\frac{2c}{\omega_p}\right)^2}}. \quad (4)$$

Here, ω_p is the plasma frequency and is taken as that of bulk silver.[19] $\hbar$ is the reduced Plank's constant, c is the speed of light in vacuum, and t is the tunnel gap (dye layer thickness). The real part of the Eigenvalues obtained after diagonalizing Eq. (2) is used to fit the spectral positions of the hybrid modes, and the results are shown in Fig. 3(c) (brown continuous curve passing through the experimental data points). The extracted thicknesses of the dye layer and silver layer are found to be ~280 nm and ~42 nm, respectively. The dashed lines in Fig. 3(a) show the uncoupled dispersions used for the fit that clearly match with the observed dispersion.

Localization of the middle hybrid mode can be thought of as analogous to the localization of electronic states in condensed matter, for example, in the Kondo insulator or Mott insulator. The interaction results in a quasi-polariton mode whose dispersion relation is modified by the interaction. The transport is determined by the derivatives of the dispersion

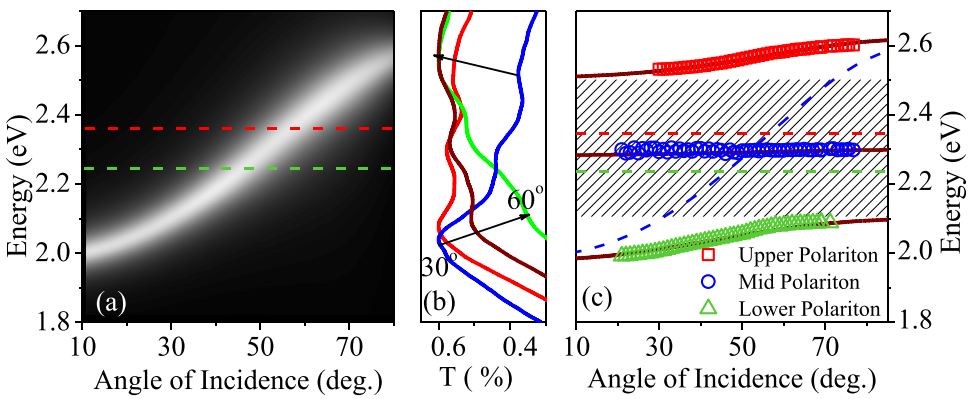

FIG. 3. (a) Mapped dispersion of the bare ASP mode. (b) Transmission spectra of the ASP-exciton hybrid system for the angle of incidence from 30° to 60°. (c) Mapped peak position showing the dispersion of the ASP-exciton hybrid modes. Dashed lines show the uncoupled mode dispersion. The brown curve shows the fit using the coupled mode model.

relation. In three mode coupling, as the dispersion gets flatter with an increase in coupling strength, the derivatives diminish and in the ultra-strong coupling limit quantities like effective mass go to infinity (inverse of the second derivative), resulting in localization. Although the flat dispersion is an indication of localization, a common signature of localization of a mode is the increase in its lifetime with a decrease in the localization length, as the out-coupling of the mode decreases for tighter localization. However, this is not true for systems with intrinsic losses, like the current one, as the largest lifetime achievable is the decay time due to the intrinsic losses. An exponentially falling tail of the mode field strength in the real space is considered to be a much more explicit signature.[6,7] But a direct measurement of the field distribution in the current configuration is impossible. Therefore, we try to provide evidence for the localization through an indirect measurement of the spatial field strength profile. We use the experimentally measured tunnel intensity to achieve the same. The intensity measured through resonant tunneling depends on the overlap between $|a_m\rangle$ and the plane wave $|k\rangle$ used for the excitation, i.e., $\langle k|a_m\rangle$. Hence, the measured intensity is directly proportional to the field strength of the mode excited during the resonant tunneling. Therefore, the transmittance at the resonance frequency of the quasi-dispersionless mode (2.29 eV) for different angles of incidence gives a measure of the field strength ($\langle k_{FD}|a_m\rangle$) for the degenerate in-plane wavelets ($|k_{FD}\rangle$), forming the quasi-dispersionless mode. The inverse Fourier transform of the same should yield the spatial field strength distribution ($\langle x|a_m\rangle$) of the same

$$\langle k|a_m\rangle = \int dk_{FD}\,\langle k|k_{FD}\rangle\langle k_{FD}|a_m\rangle = \int dk_{FD}\,\delta(k_{FD} - nk_0\sin\theta)\langle k_{FD}|a_m\rangle = \langle k_{FD}|a_m\rangle, \tag{5}$$

$$\langle x|a_m\rangle = \int dk_{FD}\,\langle x|k_{FD}\rangle\langle k_{FD}|a_m\rangle = \int dk_{FD}\,e^{ik_{FD}x}\langle k_{FD}|a_m\rangle = F\{\langle k_{FD}|a_m\rangle\}, \tag{6}$$

where $k_{FD} = nk_0\sin\theta$ and n is the refractive index of the prism.

The intensity as a function of the angle of incidence and magnitude of the in-plane wave vector has a broad maximum as shown in Figs. 4 (a) and 4(b). This results in a sharp exponential decay in real space as seen in Fig. 4(c). The localization length ξ associated with the quasi-dispersionless mode can be extracted by fitting an exponential decay of the form $I(x) = I_0\exp(-x/\xi)$, and the obtained value of ξ is 106 $\pm$ 18 nm. Interestingly, ξ obtained here is much smaller than the free space wavelength at Rabi-splitting (~535 nm). It is to be noted that exponential decays in space can also originate from losses in the system, and here these could be the losses associated with Rhodamine B absorption and plasmon propagation length (propagation loss) in silver. The length scale corresponding to the losses (length over which the intensity decays by 1/e because of losses) can be extracted from the imaginary part of the fitted Hybrid mode

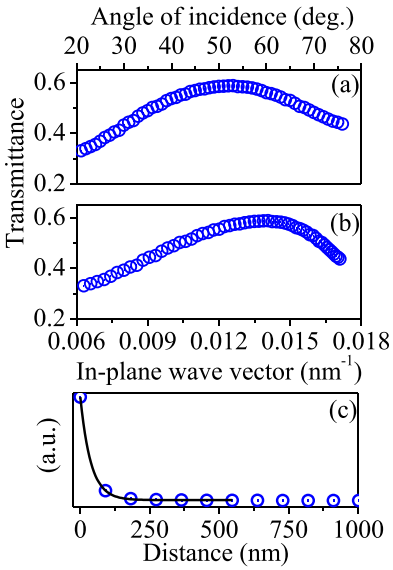

FIG. 4. (a) and (b) The measured transmittance of the middle mode (transmittance at 2.29 eV) as a function of the angle of incidence and in-plane wave vector, respectively. (c) Inverse Fourier transform of (b), showing the spatial profile of the middle mode.

Eigenvalue, and it is $5.4 \pm 0.2\,\mu$m, which is three orders larger than the obtained localization length. This clearly shows that the sharp exponential decay in Fig. 4(c) does not originate from the loss mechanisms but is due to the ultra-strong coupling induced large degeneracy that leads to the localization of the middle mode. Sub-wavelength localization close to half the wavelength is also observed in the Anderson based plasmonic system;[5] however, here the localization length is close to one fifth of the wavelength, which indicates extremely strong localization. Such a low scale for the localization length of light has been observed in geometric plasmonic localized modes alone[20] and in metallic nanoparticles.

In conclusion, we show that in the ultra-strong coupling limit, a three mode coupled system becomes irreducible, and depending on the configuration of the uncoupled modes, a localized (quasi-dispersionless) hybrid mode with interesting characteristics emerges. We experimentally implement the same with an exciton coupled cavity-plasmon system. Using a photon tunneling arrangement, we measure the dispersion and resonant tunnel intensity and show that in the ultra-strong coupling regime, a localized exciton-plasmon hybrid mode emerges with subwavelength localization and cavity plasmon-like characteristics close to Rabi splitting.

This work was facilitated by Dr. J. S. Moodera, Francis Bitter National Magnet Laboratory, Massachusetts Institute of Technology, USA, and supported by Mr. S. Gopalakrishnan, Co-founder, Infosys Technologies, India, under the Grant No. PHY/11-12/251/ALUM/SKAS.

[1]D. S. Wiersma, P. Bartolini, A. Lagendijk, and R. Righini, Nature **390**, 671 (1997).
[2]P. D. García, S. Smolka, S. Stobbe, and P. Lodahl, Phys. Rev. B **82**, 165103 (2010).
[3]S. Pandey, B. Gupta, S. Mujumdar, and A. Nahata, Light Sci. Appl. **6**, e16232 (2017).
[4]A. Farhang, N. Bigler, and O. J. F. Martin, Opt. Lett. **38**, 4758 (2013).
[5]X. Shi, X. Chen, B. A. Malomed, N. C. Panoiu, and F. Ye, Phys. Rev. B **89**, 195428 (2014).

[6]S. Mukherjee, A. Spracklen, D. Choudhury, N. Goldman, P. Öhberg, E. Andersson, and R. R. Thomson, Phys. Rev. Lett. **114**, 245504 (2015).
[7]R. A. Vicencio, C. Cantillano, L. Morales-Inostroza, B. Real, C. Mejia-Cortes, S. Weimann, A. Szameit, and M. I. Molina, Phys. Rev. Lett. **114**, 245503 (2015).
[8]K. Zhang, W. B. Shi, D. Wang, Y. Xu, R. W. Peng, R. H. Fan, Q. J. Wang, and M. Wang, Appl. Phys. Lett. **108**, 193111 (2016).
[9]O. Di Stefano, R. Stassi, L. Garziano, A. F. Kockum, S. Savasta, and F. Nori, arXiv:1603.04984v1.
[10]S. Gambino, M. Mazzeo, A. Genco, O. Di Stefano, S. Savasta, S. Patane, D. Ballarini, F. Mangione, G. Lerario, D. Sanvitto, and G. Gigli, ACS Photonics **1**, 1042 (2014).
[11]C. Weisbuch, M. Nishioka, A. Ishikawa, and Y. Arakawa, Phy. Rev. Lett. **69**, 3314 (1992).
[12]D. G. Lidzey, D. D. C. Bradley, T. Virgili, A. Armitage, M. S. Skolnick, and S. Walker, Phys. Rev. Lett. **82**, 3316 (1999).
[13]W. Zhou, M. Dridi, J. Y. Suh, C. H. Kim, D. T. Co, M. R. Wasielewski, G. C. Schatz, and T. W. Odom, Nat. Nanotechnol. **8**, 506 (2013).
[14]J. A. Dionne, L. A. Sweatlock, H. A. Atwater, and A. Polman, Phys. Rev. B **73**, 035407 (2006).
[15]A. Degiron, C. Dellagiacoma, J. G. Mcilhargey, G. Shvets, O. J. F. Martin, and D. R. Smith, Opt. Lett. **32**, 2354 (2007).
[16]A. L. Smirl, J. B. Clark, E. W. Van Stryland, and B. R. Russell, J. Chem. Phys. **77**, 631 (1982).
[17]K. R. Welford and J. R. Sambles, J. Mod. Opt. **35**, 1467 (1988).
[18]S. Kena-Cohen, S. A. Maier, and D. D. C. Bradley, Adv. Opt. Mater. **1**, 827 (2013).
[19]P. B. Johnson and R. W. Christy, Phys. Rev. B **6**, 4370 (1972).
[20]E. Hutter and J. H. Fendler, Adv. Mater. **16**, 1685 (2004).